

# Temperature effects on the nuclear symmetry energy and symmetry free energy with an isospin and momentum dependent interaction

Jun Xu,<sup>1</sup> Lie-Wen Chen,<sup>1,2</sup> Bao-An Li,<sup>3</sup> and Hong-Ru Ma<sup>1</sup>

<sup>1</sup>*Institute of Theoretical Physics, Shanghai Jiao Tong University, Shanghai 200240, China*

<sup>2</sup>*Center of Theoretical Nuclear Physics, National Laboratory of Heavy-Ion Accelerator, Lanzhou, 730000, China*

<sup>3</sup>*Department of Physics, Texas A&M University-Commerce, Commerce,*

*TX 75429, and Department of Chemistry and Physics, P.O. Box 419,*

*Arkansas State University, State University, AR 72467-0419, USA*

Within a self-consistent thermal model using an isospin and momentum dependent interaction (MDI) constrained by the isospin diffusion data in heavy-ion collisions, we investigate the temperature dependence of the symmetry energy  $E_{sym}(\rho, T)$  and symmetry free energy  $F_{sym}(\rho, T)$  for hot, isospin asymmetric nuclear matter. It is shown that the symmetry energy  $E_{sym}(\rho, T)$  generally decreases with increasing temperature while the symmetry free energy  $F_{sym}(\rho, T)$  exhibits opposite temperature dependence. The decrement of the symmetry energy with temperature is essentially due to the decrement of the potential energy part of the symmetry energy with temperature. The difference between the symmetry energy and symmetry free energy is found to be quite small around the saturation density of nuclear matter. While at very low densities, they differ significantly from each other. In comparison with the experimental data of temperature dependent symmetry energy extracted from the isotopic scaling analysis of intermediate mass fragments (IMF's) in heavy-ion collisions, the resulting density and temperature dependent symmetry energy  $E_{sym}(\rho, T)$  is then used to estimate the average freeze-out density of the IMF's.

PACS numbers: 25.70.-z, 21.65.+f, 21.30.Fe, 24.10.Pa

## I. INTRODUCTION

The equation of state (EOS) of isospin asymmetric nuclear matter, especially the nuclear symmetry energy, is essential in understanding not only many aspects of nuclear physics, but also a number of important issues in astrophysics [1, 2, 3, 4, 5, 6, 7, 8, 9]. Information about the symmetry energy at zero temperature is important for determining ground state properties of exotic nuclei and properties of cold neutron stars at  $\beta$ -equilibrium, while the symmetry energy or symmetry free energy of hot neutron-rich matter is important for understanding the liquid-gas phase transition of asymmetric nuclear matter, the dynamical evolution of massive stars and the supernova explosion mechanisms. Heavy-ion reactions induced by neutron-rich nuclei provide a unique means to investigate the symmetry energy [1, 2, 7]. In particular, recent analyses of the isospin diffusion data in heavy-ion reactions [10, 11, 12] have already put a stringent constraint on the symmetry energy of cold neutron-rich matter at sub-normal densities. On the other hand, the temperature dependence of the symmetry energy or symmetry free energy for hot neutron-rich matter has received so far little theoretical attention [13, 14, 15].

For finite nuclei at temperatures below about 3 MeV, the shell structure and pairing as well as vibrations of nuclear surfaces are important and the symmetry energy was predicted to increase slightly with the increasing temperature [16, 17]. Interestingly, an increase by only about 8% in the symmetry energy in the range of  $T$  from 0 to 1 MeV was found to affect appreciably the physics of stellar collapse, especially the neutralization processes [16]. At higher temperatures, one expects the symme-

try energy to decrease as the Pauli blocking becomes less important when the nucleon Fermi surfaces become more diffused at increasingly higher temperatures [13, 14, 15]. Based on a simplified degenerate Fermi gas model at finite temperatures, two of present authors [15] have recently studied the temperature dependence of the symmetry energy and it was shown that the experimentally observed decrease of the nuclear symmetry energy with the increasing centrality or the excitation energy in isotopic scaling analyses of heavy-ion reactions can be well understood analytically within the degenerate Fermi gas model. In particular, it was argued that the symmetry energy extracted from isotopic scaling analyses of heavy-ion reactions reflects the symmetry energy of *bulk nuclear matter* for the emission source. Furthermore, it was found that the evolution of the symmetry energy extracted from the isotopic scaling analysis is mainly due to the variation in the freeze-out density rather than temperature when the fragments are emitted in the reactions carried out under different conditions.

In the present work, within a self-consistent thermal model using an isospin and momentum dependent interaction (MDI) constrained by the isospin diffusion data in heavy-ion collisions, we study systematically the temperature dependence of the nuclear matter symmetry energy  $E_{sym}(\rho, T)$  and symmetry free energy  $F_{sym}(\rho, T)$ . It is shown that the nuclear matter symmetry energy  $E_{sym}(\rho, T)$  generally decreases with increasing temperature while the symmetry free energy  $F_{sym}(\rho, T)$  exhibits opposite temperature dependence. The decrement of the symmetry energy with temperature is essentially due to the decrement of the potential energy part of the symmetry energy with temperature. Furthermore, the difference

between the nuclear matter symmetry energy  $E_{sym}(\rho, T)$  and symmetry free energy  $F_{sym}(\rho, T)$  is found to be quite small around nuclear saturation density. Using the resulting density and temperature dependent symmetry energy  $E_{sym}(\rho, T)$ , we estimate the average freeze-out density of the fragment emission source based on the measured temperature dependent symmetry energy from the isotopic scaling analysis in heavy-ion collisions.

The paper is organized as follows. In Section II, we introduce the isospin and momentum dependent MDI interaction and the detailed numerical method to obtain the EOS of the symmetric nuclear matter and pure neutron matter at finite temperatures. Results on the temperature dependence of the symmetry energy and symmetry free energy are presented in Section III. In Section IV, we discuss the experimental data of the isotopic scaling in heavy-ion collisions by means of the obtained density and temperature dependent symmetry energy. A summary is given in Section V.

## II. HOT NUCLEAR MATTER EOS IN MOMENTUM DEPENDENT INTERACTION

Our study is based on a self-consistent thermal model using a modified finite-range Gogny effective interaction, i.e., the isospin- and momentum-dependent MDI interaction [18]. In the MDI interaction, the potential energy density  $V(\rho, T, \delta)$  of a thermal equilibrium asymmetric nuclear matter at total density  $\rho$ , temperature  $T$  and isospin asymmetry  $\delta$  is expressed as follows [11, 18],

$$V(\rho, T, \delta) = \frac{A_u \rho_n \rho_p}{\rho_0} + \frac{A_l}{2\rho_0} (\rho_n^2 + \rho_p^2) + \frac{B}{\sigma + 1} \frac{\rho^{\sigma+1}}{\rho_0^\sigma} (1 - x\delta^2) + \frac{1}{\rho_0} \sum_{\tau, \tau'} C_{\tau, \tau'} \int \int d^3p d^3p' \frac{f_\tau(\vec{r}, \vec{p}) f_{\tau'}(\vec{r}, \vec{p}')}{1 + (\vec{p} - \vec{p}')^2 / \Lambda^2}$$

In mean field approximation, Eq. (1) leads to the following single particle potential for a nucleon with momentum  $\vec{p}$  and isospin  $\tau$  in the thermal equilibrium asymmetric nuclear matter, i.e., [11, 18]

$$U(\rho, T, \delta, \vec{p}, \tau) = A_u(x) \frac{\rho_{-\tau}}{\rho_0} + A_l(x) \frac{\rho_\tau}{\rho_0} + B \left( \frac{\rho}{\rho_0} \right)^\sigma (1 - x\delta^2) - 8\tau x \frac{B}{\sigma + 1} \frac{\rho^{\sigma-1}}{\rho_0^\sigma} \delta \rho_{-\tau} + \frac{2C_{\tau, \tau}}{\rho_0} \int d^3p' \frac{f_\tau(\vec{r}, \vec{p}')}{1 + (\vec{p} - \vec{p}')^2 / \Lambda^2} + \frac{2C_{\tau, -\tau}}{\rho_0} \int d^3p' \frac{f_{-\tau}(\vec{r}, \vec{p}')}{1 + (\vec{p} - \vec{p}')^2 / \Lambda^2}. \quad (2)$$

In the above  $\tau = 1/2$  ( $-1/2$ ) for neutrons (protons);  $\sigma = 4/3$ ;  $f_\tau(\vec{r}, \vec{p})$  is the phase space distribution function at coordinate  $\vec{r}$  and momentum  $\vec{p}$ . The parameters

$A_u(x)$ ,  $A_l(x)$ ,  $B$ ,  $C_{\tau, \tau}$ ,  $C_{\tau, -\tau}$  and  $\Lambda$  have been assumed to be temperature independent and are obtained by fitting the momentum-dependence of  $U(\rho, T = 0, \delta, \vec{p}, \tau)$  to that predicted by the Gogny Hartree-Fock and/or the Brueckner-Hartree-Fock calculations, the zero temperature saturation properties of symmetric nuclear matter and the symmetry energy of 31.6 MeV at normal nuclear matter density  $\rho_0 = 0.16 \text{ fm}^{-3}$  [18]. The incompressibility  $K_0$  of cold symmetric nuclear matter at saturation density  $\rho_0$  is set to be 211 MeV. The parameters  $A_u(x)$  and  $A_l(x)$  depend on the  $x$  parameter according to

$$A_u(x) = -95.98 - x \frac{2B}{\sigma + 1}, \quad A_l(x) = -120.57 + x \frac{2B}{\sigma + 1}. \quad (3)$$

The different  $x$  values in the MDI interaction are introduced to vary the density dependence of the nuclear symmetry energy while keeping other properties of the nuclear equation of state fixed [11] and they can be adjusted to mimic predictions on the density dependence of nuclear matter symmetry energy by microscopic and/or phenomenological many-body theories. The last two terms of Eq. (2) contain the momentum-dependence of the single-particle potential. The momentum dependence of the symmetry potential stems from the different interaction strength parameters  $C_{\tau, -\tau}$  and  $C_{\tau, \tau}$  for a nucleon of isospin  $\tau$  interacting, respectively, with unlike and like nucleons in the background fields. More specifically, we use  $C_{\tau, -\tau} = -103.4$  MeV and  $C_{\tau, \tau} = -11.7$  MeV. We note that the MDI interaction has been extensively used in the transport model for studying isospin effects in intermediate energy heavy-ion collisions induced by neutron-rich nuclei [11, 12, 19, 20, 21, 22, 23, 24]. In particular, the isospin diffusion data from NSCL/MSU have constrained the value of  $x$  to be between 0 and  $-1$  for nuclear matter densities less than about  $1.2\rho_0$  [11, 12], we will thus in the present work consider the two values of  $x = 0$  and  $x = -1$ .

At zero temperature,  $f_\tau(\vec{r}, \vec{p}) = \frac{2}{h^3} \Theta(p_f(\tau) - p)$  and the integral in Eqs. (1) and (2) can be calculated analytically [18]. For an asymmetric nuclear matter at thermal equilibrium with a finite temperature  $T$ , the phase space distribution function becomes the Fermi distribution

$$f_\tau(\vec{r}, \vec{p}) = \frac{2}{h^3} \frac{1}{\exp\left(\frac{\epsilon(\rho, T, \delta, \vec{p}, \tau) - \mu_\tau}{T}\right) + 1} \quad (4)$$

where  $\mu_\tau$  is the chemical potential and  $\epsilon(\rho, T, \delta, \vec{p}, \tau)$  is the total single particle energy for a nucleon with isospin  $\tau$  and momentum  $\vec{p}$ , which includes the kinetic energy and the single particle potential  $U(\rho, T, \delta, \vec{p}, \tau)$ , i.e.,

$$\epsilon(\rho, T, \delta, \vec{p}, \tau) = \frac{p^2}{2m_\tau} + A_u \frac{\rho_{-\tau}}{\rho_0} + A_l \frac{\rho_\tau}{\rho_0} + B \left( \frac{\rho}{\rho_0} \right)^\sigma (1 - x\delta^2) - 8\tau x \frac{B}{\sigma + 1} \frac{\rho^{\sigma-1}}{\rho_0^\sigma} \delta \rho_{-\tau} + R_{\tau, \tau}(\rho, \vec{p}) + R_{\tau, -\tau}(\rho, \vec{p}) \quad (5)$$

with

$$R_{\tau_1, \tau_2}(\rho, \vec{p}) = \frac{2C_{\tau_1, \tau_2}}{\rho_0} \int d^3p' \frac{f_{\tau_2}(\vec{r}, \vec{p}')}{1 + (\vec{p} - \vec{p}')^2/\Lambda^2} \quad (6)$$

where  $\tau_1$  and  $\tau_2$  can be chosen as the same or different to mimic the last two terms of Eq. (2).

The chemical potential  $\mu_\tau$  is therefore independent of the nucleon momentum  $\vec{p}$  and can be determined from

$$\rho_\tau = \frac{8\pi}{h^3} \int_0^\infty \frac{p^2 dp}{\exp\left(\frac{\epsilon(\rho, T, \delta, \vec{p}, \tau) - \mu_\tau}{T}\right) + 1}. \quad (7)$$

From Eq. (7), we can see that, at finite temperature, to obtain the chemical potential  $\mu_\tau$  requires knowing  $\epsilon(\rho, T, \delta, \vec{p}, \tau)$  (and thus  $R_{\tau_1, \tau_2}(\rho, \vec{p})$ ) for all  $\vec{p}$ , while from Eq. (6) knowing  $R_{\tau_1, \tau_2}(\rho, \vec{p})$  needs further to know  $f_\tau(\vec{r}, \vec{p})$  which again depends on the chemical potential  $\mu_\tau$  from Eq. (4). Therefore, Eqs. (4), (5), (6), and (7) constitute closed sets of equations whose solution can be obtained by a self-consistency iteration, just as in the Hartree-Fock theory.

Following the recipe used in Ref. [25], the self-consistency problem of Eqs. (4), (5), (6), and (7) can be solved by the following iterative scheme. Firstly, we make an initial guess for  $R_{\tau_1, \tau_2}(\rho, \vec{p})$  from the zero temperature condition, i.e.,

$$R_{\tau_1, \tau_2}^0(\rho, \vec{p}) = \frac{2C_{\tau_1, \tau_2}}{\rho_0} \int d^3p' \frac{\frac{2}{h^3} \Theta(p_f(\tau_2) - p')}{1 + (\vec{p} - \vec{p}')^2/\Lambda^2} \quad (8)$$

where  $p_f(\tau) = \hbar(3\pi^2\rho_\tau)^{1/3}$  is the Fermi momentum. The right hand side of Eq. (8) is not related to the chemical potential  $\mu_\tau$  and thus the initial form of the single nucleon energy  $\epsilon^0(\rho, T, \delta, \vec{p}, \tau)$  can be obtained. Secondly, substitute  $\epsilon^0(\rho, T, \delta, \vec{p}, \tau)$  into Eq. (7) to obtain the initial chemical potential  $\mu_\tau^0$  for protons and neutrons. Then, use  $\epsilon^0(\rho, T, \delta, \vec{p}, \tau)$  and  $\mu_\tau^0$  to obtain new  $R_{\tau_1, \tau_2}(\rho, \vec{p})$  function, namely,  $R_{\tau_1, \tau_2}^1(\rho, \vec{p})$  from Eq. (4) and (6). This in turn gives the new single nucleon energy  $\epsilon^1(\rho, T, \delta, \vec{p}, \tau)$  from Eq. (5) and then the new chemical potential  $\mu_\tau^1$  can be obtained from Eq. (7). The cycle is repeated and a few iterations are sufficient to achieve convergence for the chemical potential  $\mu_\tau$  with enough accuracy. It should be mentioned that the neutron and proton chemical potentials are coupled with each other in asymmetric nuclear matter and thus the convergence condition must be satisfied simultaneously for neutrons and protons.

With the self-consistency iteration, we can finally obtain the chemical potential  $\mu_\tau$  and the single nucleon energy  $\epsilon(\rho, T, \delta, \vec{p}, \tau)$  for an asymmetric nuclear matter at thermal equilibrium with a finite temperature  $T$ . The potential energy density  $V(\rho, T, \delta)$  of the thermal equilibrium asymmetric nuclear matter then can be calculated from Eq. (1) and the energy per nucleon  $E(\rho, T, \delta)$  is then obtained as

$$E(\rho, T, \delta) = \frac{1}{\rho} \left[ V(\rho, T, \delta) + \sum_\tau \int d^3p \frac{p^2}{2m_\tau} f_\tau(\vec{r}, \vec{p}) \right]. \quad (9)$$

Furthermore, we can obtain the entropy per nucleon  $S_\tau(\rho, T, \delta)$  of the thermal equilibrium asymmetric nuclear matter as

$$S_\tau(\rho, T, \delta) = -\frac{8\pi}{\rho h^3} \int_0^\infty p^2 [n_\tau \ln n_\tau + (1-n_\tau) \ln(1-n_\tau)] dp \quad (10)$$

with the occupation probability

$$n_\tau = \frac{1}{\exp\left(\frac{\epsilon(\rho, T, \delta, \vec{p}, \tau) - \mu_\tau}{T}\right) + 1}. \quad (11)$$

Finally, the free energy per nucleon  $F(\rho, T, \delta)$  of the thermal equilibrium asymmetric nuclear matter can be obtained from the thermodynamic relation

$$F(\rho, T, \delta) = E(\rho, T, \delta) - T \sum_\tau S_\tau(\rho, T, \delta). \quad (12)$$

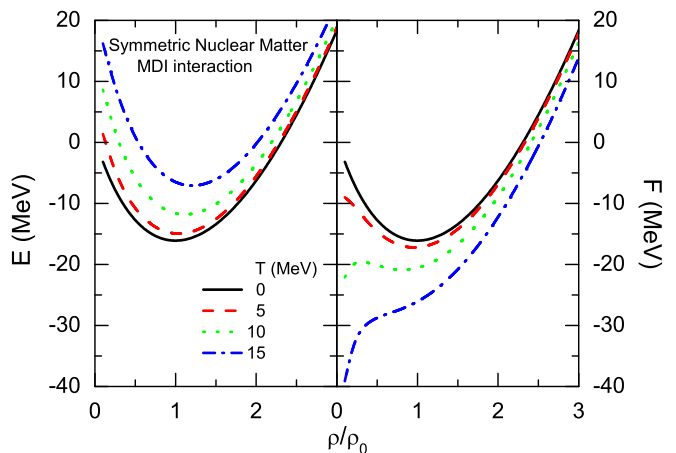


FIG. 1: (Color online) Density dependence of the energy per nucleon  $E$  (left panel) and free energy per nucleon  $F$  (right panel) for symmetric nuclear matter at  $T = 0$  MeV, 5 MeV, 10 MeV and 15 MeV with the MDI interaction.

Using the MDI interaction, we can now calculate the energy per nucleon  $E(\rho, T, \delta)$  and free energy per nucleon  $F(\rho, T, \delta)$  of nuclear matter at finite temperature from Eq. (9) and (12). Shown in Fig. 1 is the density dependence of  $E(\rho, T, \delta)$  and  $F(\rho, T, \delta)$  for symmetric nuclear matter at  $T = 0$  MeV, 5 MeV, 10 MeV and 15 MeV using the MDI interaction with  $x = 0$  and  $-1$ . For symmetric nuclear matter ( $\delta = 0$ ), the parameter  $x = 0$  would give the same results as the parameter  $x = -1$  as we have discussed above, and thus the curves shown in Fig. 1 are the same for  $x = 0$  and  $-1$ . From Fig. 1, one can see that the energy per nucleon  $E(\rho, T, \delta)$  increases with increasing temperature  $T$  while the free energy per nucleon  $F(\rho, T, \delta)$  decreases with increment of  $T$ . The increment of the energy per nucleon  $E(\rho, T, \delta)$  with the temperature reflects the thermal excitation of the nuclear matter due to the change of the phase-space distribution function

$f_\tau(\vec{r}, \vec{p})$ . With the increment of the temperature, more nucleons move to higher momentum states and thus lead to larger internal energy per nucleon. On the other hand, the decrement of the free energy per nucleon  $F(\rho, T, \delta)$  with  $T$  is mainly due to the increment of the entropy per nucleon with increasing temperature. This feature also implies that the increment of  $TS(\rho, T)$  with  $T$  is larger than the increment of  $E(\rho, T)$  with  $T$ . Furthermore, the temperature effects are seen to be stronger at lower densities while they become much weaker at higher densities. At lower densities, the Fermi momentum  $p_f(\tau)$  is smaller and thus temperature effects on the energy per nucleon  $E(\rho, T, \delta)$  are expected to be stronger. Meanwhile, the entropy per nucleon becomes larger at lower densities where the particles become more free in phase space and thus leads to a smaller free energy per nucleon.

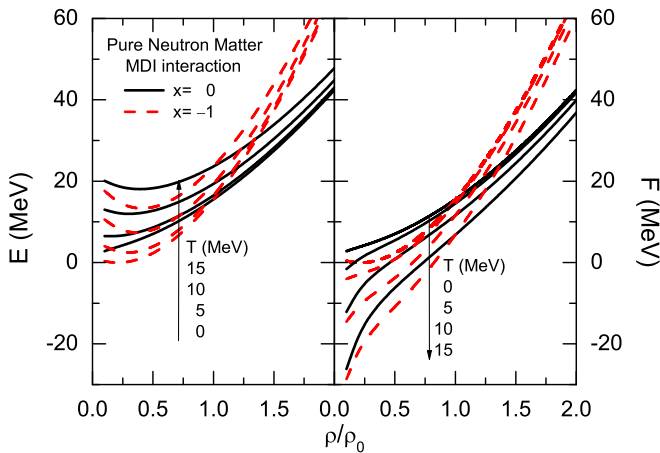


FIG. 2: (Color online) Same as Fig. 1 but for pure neutron matter using the MDI interaction with  $x = 0$  (solid lines) and  $-1$  (dashed lines).

Similarly, shown in Fig. 2 are the density dependence of the  $E(\rho, T, \delta)$  and  $F(\rho, T, \delta)$  for pure neutron matter at  $T = 0$  MeV, 5 MeV, 10 MeV and 15 MeV using the MDI interaction with  $x = 0$  and  $-1$ . The temperature dependence of the  $E(\rho, T, \delta)$  and  $F(\rho, T, \delta)$  for pure neutron matter is seen to be similar to that of the symmetric nuclear matter as shown in Fig. 1. However, the parameters  $x = 0$  and  $-1$  display different density dependence for the energy per nucleon  $E(\rho, T, \delta)$  and free energy per nucleon  $F(\rho, T, \delta)$ , which just reflects that the parameters  $x = 0$  and  $-1$  give different density dependence of the nuclear symmetry energy and symmetry free energy as will be discussed in the following.

### III. NUCLEAR SYMMETRY ENERGY AND SYMMETRY FREE ENERGY

As in the case of zero temperature, phenomenological and microscopic studies [13, 14] indicate that the

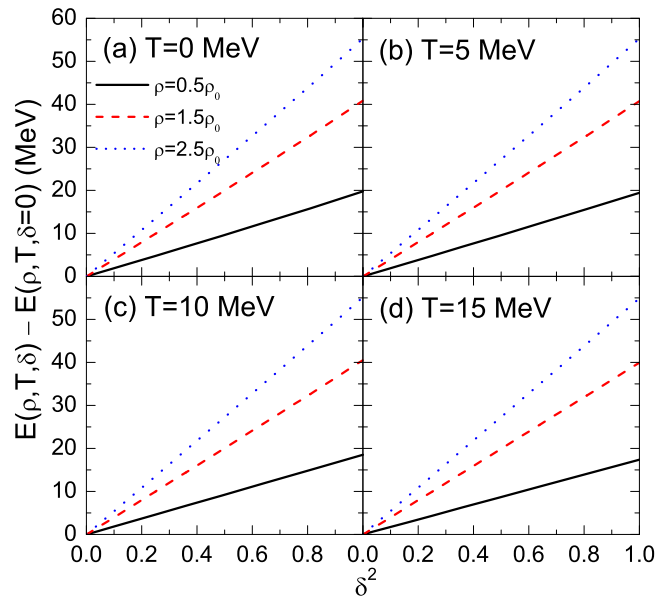


FIG. 3: (Color online)  $E(\rho, T, \delta) - E(\rho, T, \delta = 0)$  as a function of  $\delta^2$  at temperature  $T = 0$  MeV (a), 5 MeV (b), 10 MeV (c) and 15 MeV (d) for three different baryon number densities  $\rho = 0.5\rho_0, 1.5\rho_0$  and  $2.5\rho_0$  using the MDI interaction with  $x = 0$ .

equation of state of hot neutron-rich matter at density  $\rho$ , temperature  $T$ , and an isospin asymmetry  $\delta$  can also be written as a parabolic function of  $\delta$ , i.e.,

$$E(\rho, T, \delta) = E(\rho, T, \delta = 0) + E_{sym}(\rho, T)\delta^2 + \mathcal{O}(\delta^4). \quad (13)$$

The temperature and density dependent symmetry energy  $E_{sym}(\rho, T)$  for hot neutron-rich matter can thus be extracted from  $E_{sym}(\rho, T) \approx E(\rho, T, \delta = 1) - E(\rho, T, \delta = 0)$ . The symmetry energy  $E_{sym}(\rho, T)$  is the energy cost to convert all protons in symmetry matter to neutrons at the fixed temperature  $T$  and density  $\rho$ . In order to check the empirical parabolic law Eq. (13) for the MDI interaction, we show in Fig. 3  $E(\rho, T, \delta) - E(\rho, T, \delta = 0)$  as a function of  $\delta^2$  at temperature  $T = 0$  MeV, 5 MeV, 10 MeV and 15 MeV for three different baryon number densities  $\rho = 0.5\rho_0, 1.5\rho_0$  and  $2.5\rho_0$  using the MDI interaction with  $x = 0$ . The clear linear relation between  $E(\rho, T, \delta) - E(\rho, T, \delta = 0)$  and  $\delta^2$  shown in Fig. 3 indicates the validity of the empirical parabolic law Eq. (13) for the hot neutron-rich matter. We note that the empirical parabolic law Eq. (13) is also well satisfied for the parameter  $x = -1$ .

Similarly, we can define the symmetry free energy  $F_{sym}(\rho, T)$  by the following parabolic approximation to the free energy per nucleon

$$F(\rho, T, \delta) = F(\rho, T, \delta = 0) + F_{sym}(\rho, T)\delta^2 + \mathcal{O}(\delta^4). \quad (14)$$

The temperature and density dependent symmetry free energy  $F_{sym}(\rho, T)$  for hot neutron-rich matter can thus be extracted from  $F_{sym}(\rho, T) \approx F(\rho, T, \delta = 1) -$



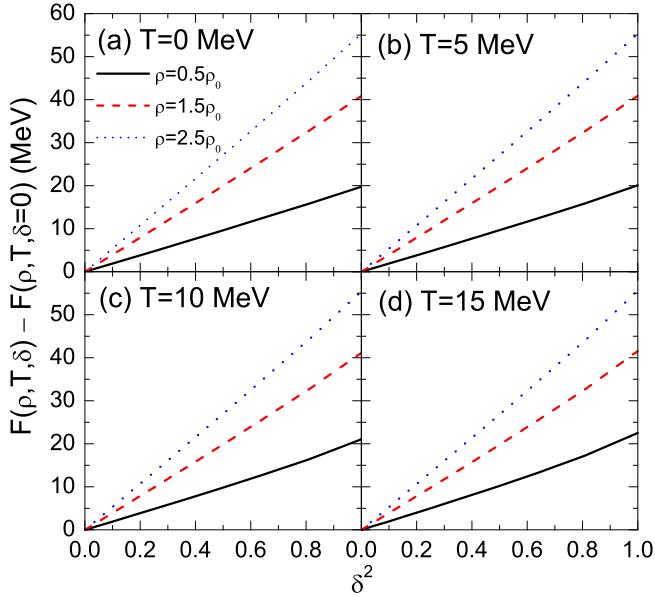


FIG. 4: (Color online) Same as Fig. 3 but for the free energy per nucleon  $F(\rho, T, \delta)$ .

$F(\rho, T, \delta = 0)$  which is just the free energy cost to convert all protons in symmetry matter to neutrons at the fixed temperature  $T$  and density  $\rho$ . In order to check if the empirical parabolic law is also valid for the free energy per nucleon of hot neutron-rich matter, we show in Fig. 4  $F(\rho, T, \delta) - F(\rho, T, \delta = 0)$  as a function of  $\delta^2$  at temperature  $T = 0$  MeV, 5 MeV, 10 MeV and 15 MeV for three different baryon number densities  $\rho = 0.5\rho_0, 1.5\rho_0$  and  $2.5\rho_0$  using the MDI interaction with  $x = 0$ . One can see from Fig. 4 that the parabolic law Eq. (14) is also approximately satisfied though at low densities and high temperatures, the linear relation between  $F(\rho, T, \delta) - F(\rho, T, \delta = 0)$  and  $\delta^2$  is violated slightly. For the parameter  $x = -1$ , we also obtained the similar conclusion.

In Fig. 5, we show the density dependence of the symmetry energy  $E_{sym}(\rho, T)$  and the symmetry free energy  $F_{sym}(\rho, T)$  at  $T = 0$  MeV, 5 MeV, 10 MeV and 15 MeV using the MDI interaction with  $x = 0$  and  $-1$ . For different choice of the parameter  $x = 0$  and  $-1$ ,  $E_{sym}(\rho, T)$  and  $F_{sym}(\rho, T)$  display different density dependence with  $x = 0$  ( $-1$ ) giving larger (smaller) values for the symmetry energy and the symmetry free energy at lower densities while smaller (larger) ones at higher densities for a fixed temperature. Similar to the  $E(\rho, T, \delta)$  and  $F(\rho, T, \delta)$  as shown in Figs. 1 and 2, the temperature effects on the symmetry energy  $E_{sym}(\rho, T)$  and the symmetry free energy  $F_{sym}(\rho, T)$  are found to be stronger at lower densities while they become much weaker at higher densities.

Interestingly, we can see from Fig. 5 that the symmetry energy  $E_{sym}(\rho, T)$  and the symmetry free energy  $F_{sym}(\rho, T)$  exhibit opposite temperature dependence,

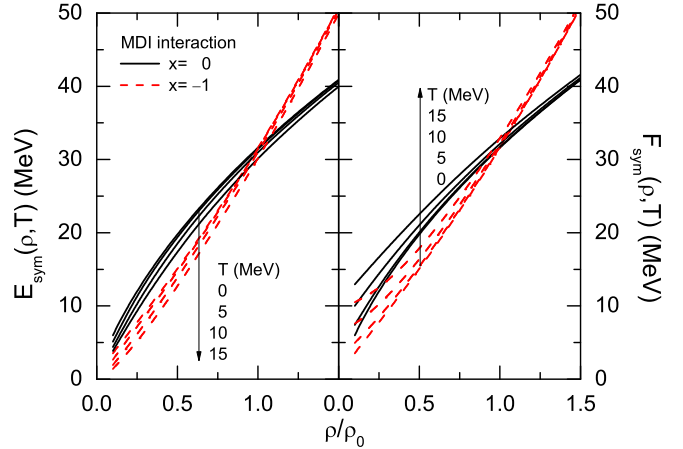


FIG. 5: (Color online) Density dependence of the symmetry energy  $E_{sym}(\rho, T)$  (left panel) and the symmetry free energy  $F_{sym}(\rho, T)$  (right panel) at  $T = 0$  MeV, 5 MeV, 10 MeV and 15 MeV using the MDI interaction with  $x = 0$  and  $-1$ .

namely, with increasing temperature  $T$ ,  $E_{sym}(\rho, T)$  decreases while  $F_{sym}(\rho, T)$  increases. This also means that  $F_{sym}(\rho, T)$  always has larger values than  $E_{sym}(\rho, T)$  at fixed density and temperature since they are identical at zero temperature. At higher temperatures, one expects the symmetry energy  $E_{sym}(\rho, T)$  to decrease as the Pauli blocking (a pure quantum effect) becomes less important when the nucleon Fermi surfaces become more diffused at increasingly higher temperatures [13, 14, 15]. On the other hand, the symmetry free energy  $F_{sym}(\rho, T)$  is related to the entropy per nucleon of the asymmetric nuclear matter, which is not a pure quantum effect, and its increment with increasing temperature can be understood by the following expression

$$\begin{aligned}
 F_{sym}(\rho, T) &= E_{sym}(\rho, T) \\
 &\quad + T [S_n(\rho, T, \delta = 0) + S_p(\rho, T, \delta = 0)] \\
 &\quad - T S_n(\rho, T, \delta = 1).
 \end{aligned}
 \tag{15}$$

The first term of the right hand side in Eq. (15) is the symmetry energy  $E_{sym}(\rho, T)$ , which decreases with increasing temperature as discussed above. However, the total entropy per nucleon of the symmetric nuclear matter is larger than that of the pure neutron matter and their difference becomes larger with increasing temperature, which leads to a positive value for the difference between the last two terms of the right hand side in Eq. (15). Therefore,  $F_{sym}(\rho, T)$  has larger values than  $E_{sym}(\rho, T)$  at fixed density and temperature. Furthermore, the increment of  $TS(\rho, T)$  with  $T$  is stronger than the increment of  $E(\rho, T)$  with  $T$  as mentioned above, and the combinational effects thus cause the symmetry free energy  $F_{sym}(\rho, T)$  increase with increasing temperature.

Within the present self-consistent thermal model, because the single particle potential is momentum dependent with the MDI interaction, the potential part of the

symmetry energy is expected to be temperature dependent. It is thus interesting to study how the potential and kinetic parts of the symmetry energy  $E_{sym}(\rho, T)$  may vary respectively with temperature. However, for the symmetry free energy  $F_{sym}(\rho, T)$ , one cannot separate its potential and kinetic parts since  $F_{sym}(\rho, T)$  depends on the entropy that is determined by the phase space distribution function. Fig. 6 displays the temperature dependence of the symmetry energy  $E_{sym}(\rho, T)$  as well as its potential and kinetic energy parts using the MDI interaction with  $x = 0$  at  $\rho = \rho_0$ ,  $0.5\rho_0$ , and  $0.1\rho_0$ . With the parameter  $x = -1$ , the same conclusion is obtained. It is seen that both the symmetry energy  $E_{sym}(\rho, T)$  and its potential energy part decrease with increasing temperature at all three densities considered. While the kinetic energy part of the  $E_{sym}(\rho, T)$  increases slightly with increasing temperature for  $\rho = \rho_0$  and  $0.5\rho_0$  and decreases for  $\rho = 0.1\rho_0$ . These features are uniquely determined by the momentum dependence in the MDI interaction within the present self-consistent thermal model. The decrement of the kinetic energy part of the symmetry energy with temperature at very low densities is consistent with predictions of the Fermi gas model at high temperatures and/or very low densities [15, 26]. In the study of Ref. [15] using the simplified degenerate Fermi gas model the potential part of the symmetry energy was assumed to be temperature independent for simplicity. The decrease of the symmetry energy observed there is thus completely due to the decrease in the kinetic contribution. However, we note that the temperature dependence of the total symmetry energy  $E_{sym}(\rho, T)$  is consistent with each other for the two models. This is due to the fact that the phase space distribution function will vary self-consistently according to if the single particle potential is or not momentum dependent. From the present self-consistent thermal model with momentum dependent MDI interaction, our results indicate that the decreasing symmetry energy with increasing temperature is essentially due to the decrement of its potential contribution.

#### IV. ISOTOPIC SCALING IN HEAVY-ION COLLISIONS

It has been observed experimentally and theoretically in many types of reactions that the ratio  $R_{21}(N, Z)$  of yields of a fragment with proton number  $Z$  and neutron number  $N$  from two reactions reaching about the same temperature  $T$  satisfies an exponential relationship  $R_{21}(N, Z) \propto \exp(\alpha N)$  [27, 28, 29, 30, 31, 32, 33, 34, 35, 36, 37, 38]. Particularly, in several statistical and dynamical models under some assumptions [34, 35, 36], it has been shown that the scaling coefficient  $\alpha$  is related to the symmetry energy  $C_{sym}(\rho, T)$  via

$$\alpha = \frac{4C_{sym}(\rho, T)}{T} \Delta [(Z/A)^2], \quad (16)$$

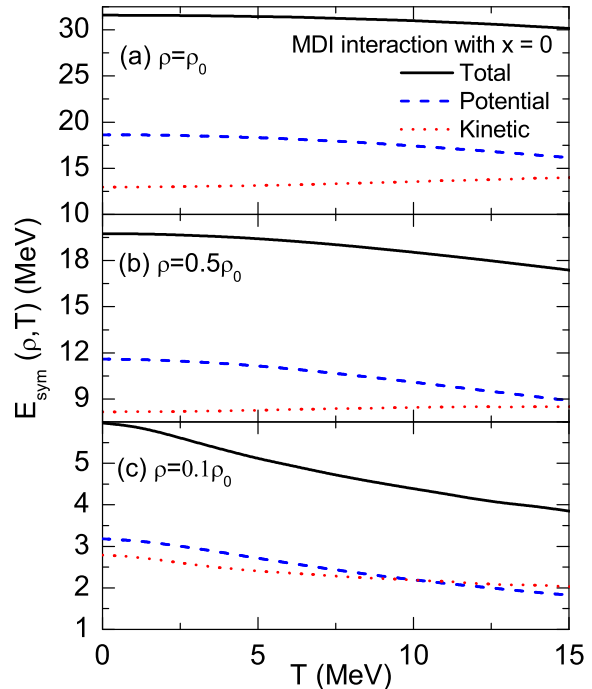


FIG. 6: (Color online) Temperature dependence of the symmetry energy  $E_{sym}(\rho, T)$  as well as its potential energy part and kinetic energy part using MDI interaction with  $x = 0$  at  $\rho = \rho_0$  (a),  $0.5\rho_0$  (b), and  $0.1\rho_0$  (c).

where  $\Delta[(Z/A)^2] \equiv (Z_1/A_1)^2 - (Z_2/A_2)^2$  is the difference between the  $(Z/A)^2$  values of the two fragmenting sources created in the two reactions.

As mentioned in Ref. [15], however, because of the different assumptions used in the various derivations, the validity of Eq. (16) is still disputable as to whether and when the  $C_{sym}$  is actually the symmetry energy or the symmetry free energy. Moreover, the physical interpretation of the  $C_{sym}(\rho, T)$  is also not clear, sometimes even contradictory, in the literature. The main issue is whether the  $C_{sym}$  measures the symmetry energy of the fragmenting source or that of the fragments formed at freeze-out. This ambiguity is also due to the fact that the derivation of Eq. (16) is not unique. In particular, within the grand canonical statistical model for multifragmentation [34, 35] the  $C_{sym}$  refers to the symmetry energy of primary fragments. While within the sequential Weisskopf model in the grand canonical limit [34] it refers to the symmetry energy of the emission source. Following the arguments in Ref. [15], we assume in the present work that the  $C_{sym}$  reflects the symmetry energy of *bulk nuclear matter* for the emission source.

In Fig. 7, we show the symmetry energy  $E_{sym}(\rho, T)$  and symmetry free energy  $F_{sym}(\rho, T)$  as a function of temperature using MDI interaction with  $x = 0$  and  $-1$  at different densities from  $0.1\rho_0$  to  $\rho_0$ . The temperature dependence of the symmetry energy  $E_{sym}(\rho, T)$  is seen to be very similar to that in Ref. [15] where a simplified de-

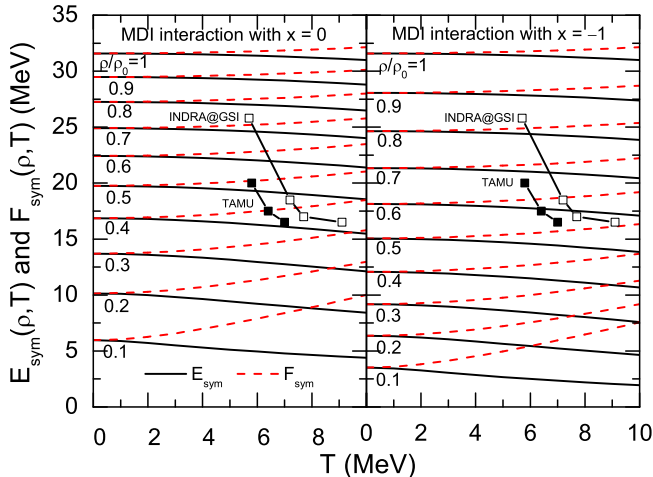


FIG. 7: (Color online) Temperature dependence of the symmetry energy (solid lines) and symmetry free energy (dashed lines) using MDI interaction with  $x = 0$  (left panel) and  $-1$  (right panel) at different densities from  $0.1\rho_0$  to  $\rho_0$ . The experimental data from Texas A&M University (solid squares) and the INDRA-ALADIN collaboration at GSI (open squares) are included for comparison.

generate Fermi gas model at finite temperatures has been used. The symmetry energy does not change much with the temperature at a given density, especially around the saturation density  $\rho_0$ . Furthermore, it is seen that while the symmetry energy  $E_{sym}(\rho, T)$  decreases slightly with the increasing temperature at a given density, the symmetry free energy  $F_{sym}(\rho, T)$  increases instead. Around the saturation density  $\rho_0$ , it is found that the difference between the symmetry energy  $E_{sym}(\rho, T)$  and the symmetry free energy  $F_{sym}(\rho, T)$  is quite small, i.e., only several percents, though at higher temperature, compared with their values at  $T = 0$  MeV. This feature confirms the assumption on identifying  $C_{sym}(\rho, T)$  to  $E_{sym}(\rho, T)$  at lower temperatures and not so low densities [28, 29, 30]. At low densities, on the other hand, the symmetry free energy  $F_{sym}(\rho, T)$  exhibits a stronger temperature dependence and it is significantly larger than the symmetry energy  $E_{sym}(\rho, T)$  at moderate and high temperatures. This is due to the fact that the entropy contribution to the symmetry free energy  $F_{sym}(\rho, T)$  becomes stronger at low densities as mentioned in Sec. II and Sec. III. It should be noted that, at low densities the entropy may be affected strongly by the clustering effects [33, 39] which are not included in the present work.

Experimentally, the temperature  $T$  and scaling coefficient  $\alpha$  (thus the  $C_{sym}$ ) of the fragment emission source can be directly measured while the determination of the density of emission source usually depends on the model used. Also included in Fig. 7 are the experimental data of the measured temperature dependent symmetry energy from Texas A&M University (TAMU) (solid squares) [30] and the INDRA-ALADIN collaboration at GSI (open

squares) [31, 32]. From Fig. 7, it is seen clearly that the experimentally observed evolution of the symmetry energy is mainly due to the change in density rather than temperature, as shown in Ref. [15]. Meanwhile, we can estimate from Fig. 7 the average freeze-out density of the fragment emission source from the measured temperature dependent symmetry energy based on the isotopic scaling analysis in heavy-ion collisions. In particular, using the symmetry energy  $E_{sym}(\rho, T)$  from the MDI interaction with  $x = 0$ , we find the average freeze-out density of the fragment emission source  $\rho_f$  is between about  $0.41\rho_0$  and  $0.52\rho_0$  for TAMU data while about  $0.42\rho_0$  and  $0.75\rho_0$  for INDRA-ALADIN collaboration data. On the other hand, using the symmetry energy  $E_{sym}(\rho, T)$  from the MDI interaction with  $x = -1$ , the  $\rho_f$  is found to be between about  $0.57\rho_0$  and  $0.68\rho_0$  for TAMU data while about  $0.58\rho_0$  and  $0.84\rho_0$  for INDRA-ALADIN collaboration data. It is interesting to see that the extracted values of  $\rho_f$  from the MDI interaction with  $x = 0$  is very similar to those extracted in Ref. [30] using different models.

Furthermore, if the symmetry free energy  $F_{sym}(\rho, T)$  from the MDI interaction with  $x = 0$  is used to estimate the  $\rho_f$ , we find the  $\rho_f$  is between about  $0.36\rho_0$  and  $0.49\rho_0$  for TAMU data and about  $0.33\rho_0$  and  $0.72\rho_0$  for INDRA-ALADIN collaboration data. While if the symmetry free energy  $F_{sym}(\rho, T)$  from the MDI interaction with  $x = -1$  is used, the  $\rho_f$  is between about  $0.52\rho_0$  and  $0.66\rho_0$  for TAMU data and about  $0.51\rho_0$  and  $0.83\rho_0$  for INDRA-ALADIN collaboration data. Therefore, the extracted  $\rho_f$  values are not sensitive to if the measured  $C_{sym}(\rho, T)$  is the symmetry energy or the symmetry free energy. However, the extracted  $\rho_f$  values are indeed sensitive to the  $x$  parameter used in the MDI interaction, namely, the density dependence of the symmetry energy. We note that the zero-temperature symmetry energy for the MDI interaction with  $x = 0$  and  $-1$  can be parameterized, respectively, as  $31.6(\rho/\rho_0)^{0.69}$  MeV and  $31.6(\rho/\rho_0)^{1.05}$  MeV [11]. Therefore, the isotopic scaling in heavy-ion collisions provides a potential good probe for the density dependence of the nuclear matter symmetry energy once the average density of the emission source has been determined in the isotopic scaling measurement, as pointed out in Ref. [15].

## V. SUMMARY

Within a self-consistent thermal model using the isospin and momentum dependent MDI interaction with  $x = 0$  and  $-1$  constrained by the isospin diffusion data in heavy-ion collisions, we have investigated the temperature dependence of the nuclear matter symmetry energy  $E_{sym}(\rho, T)$  and symmetry free energy  $F_{sym}(\rho, T)$ . It is shown that the nuclear matter symmetry energy  $E_{sym}(\rho, T)$  generally decreases with increasing temperature while the symmetry free energy  $F_{sym}(\rho, T)$  exhibits opposite temperature dependence. The decrement of the symmetry energy with temperature is essentially due to

the decrement of the potential energy part of the symmetry energy with temperature. The temperature effects on the nuclear matter symmetry energy and symmetry free energy are found to be stronger at lower densities while become much weaker at higher densities. Furthermore, the difference between the nuclear matter symmetry energy  $E_{sym}(\rho, T)$  and symmetry free energy  $F_{sym}(\rho, T)$  is found to be quite small around nuclear saturation density, although significantly large at very low densities.

Comparing the theoretical density and temperature dependent symmetry energy  $E_{sym}(\rho, T)$  with the  $C_{sym}(\rho, T)$  parameter extracted from the isotopic scaling data from TAMU and the INDRA-ALADIN collaboration at GSI, we found that the experimentally observed evolution of the symmetry energy is mainly due to the change in density rather than temperature, as shown in the previous work [15]. Meanwhile, we have estimated the average freeze-out density of the fragment emission source formed in these reactions by comparing the calculated  $E_{sym}(\rho, T)$  or  $F_{sym}(\rho, T)$  with the measured  $C_{sym}(\rho, T)$ . Our results indicate that the extracted average freeze-out densities are not sensitive to whether the experimentally measured  $C_{sym}(\rho, T)$  parameter is the symmetry energy  $E_{sym}(\rho, T)$  or the symmetry free en-

ergy  $F_{sym}(\rho, T)$  in the temperature and density ranges reached in the TAMU and INDRA/GSI experiments. They are, however, sensitive to the  $x$  parameter used in the MDI interaction, namely, the density dependence of the symmetry energy. Therefore the isotopic scaling in heavy-ion collisions provides a potentially good probe for the density dependence of the nuclear matter symmetry energy provided the average density of the emission source can be determined simultaneously in the isotopic scaling measurements.

### Acknowledgments

This work was supported in part by the National Natural Science Foundation of China under Grant Nos. 10334020, 10575071, and 10675082, MOE of China under project NCET-05-0392, Shanghai Rising-Star Program under Grant No. 06QA14024, the SRF for ROCS, SEM of China, the US National Science Foundation under Grant Nos. PHY-0652548 and PHY-0456890, and the NASA-Arkansas Space Grants Consortium Award ASU15154.

- 
- [1] B.A. Li, C.M. Ko, and W. Bauer, topical review, Int. Jour. Mod. Phys. E **7**, 147 (1998).
  - [2] *Isospin Physics in Heavy-Ion Collisions at Intermediate Energies*, Eds.. Bao-An Li and W. Udo Schröder (Nova Science Publishers, Inc, New York, 2001).
  - [3] I. Bombaci, in [2], p.35.
  - [4] A.E.L. Dieperink, Y. Dewulf, D. Van Neck, M. Waroquier, and V. Rodin, Phys. Rev. C **68**, 064307 (2003).
  - [5] P. Danielewicz, R. Lacey, and W.G. Lynch, Science **298**, 1592 (2002).
  - [6] J.M. Lattimer and M. Prakash, Phys. Rep. **333**, 121 (2000); Astrophys. J. **550**, 426 (2001); Science **304**, 536 (2004).
  - [7] V. Baran, M. Colonna, V. Greco, and M. Di Toro, Phys. Rep. **410**, 335 (2005).
  - [8] A.W. Steiner, M. Prakash, J.M. Lattimer, and P.J. Ellis, Phys. Rep. **411**, 325 (2005).
  - [9] B.A. Li and A.W. Steiner, Phys. Lett. **B642**, 436 (2006).
  - [10] M.B. Tsang *et al.*, Phys. Rev. Lett. **92**, 062701 (2004).
  - [11] L.W. Chen, C.M. Ko, and B.A. Li, Phys. Rev. Lett. **94**, 032701 (2005) [arXiv:nucl-th/0407032].
  - [12] B.A. Li and L.W. Chen, Phys. Rev. C **72**, 064611 (2005).
  - [13] L.W. Chen, F.S. Zhang, Z.H. Lu, W.F. Li, Z.Y. Zhu, and H.R. Ma, J. Phys. G **27**, 1799 (2001).
  - [14] W. Zuo *et al.*, Phys. Rev. C **69**, 064001 (2003); *ibid.* C **73**, 035208 (2006).
  - [15] B.A. Li and L.W. Chen, Phys. Rev. C **74**, 034610 (2006).
  - [16] P. Donati, P.M. Pizzochero, P.F. Bortignon, and R.A. Broglia, Phys. Rev. Lett. **72**, 2835 (1994).
  - [17] D.J. Dean, S.E. Koonin, K. Langanke, and P.B. Radha, Phys. Lett. **B356**, 429 (1995); D.J. Dean, K. Langanke, and J.M. Sampaio, Phys. Rev. C **66**, 045802 (2002).
  - [18] C. B. Das, S. Das Gupta, C. Gale and B.A. Li, Phys. Rev. C **67**, 034611 (2003).
  - [19] B.A. Li, C. B. Das, S. Das Gupta, and C. Gale, Phys. Rev. C **69**, 011603(R) (2004); Nucl. Phys. **A735**, 563 (2004).
  - [20] L.W. Chen, C.M. Ko, and B.A. Li, Phys. Rev. C **69**, 054606 (2004).
  - [21] B.A. Li, G.C. Yong, and W. Zuo, Phys. Rev. C **71**, 014608 (2005); *ibid.* C **71**, 044604 (2005).
  - [22] B.A. Li, L.W. Chen, G.C. Yong, and W. Zuo, Phys. Lett. **B634**, 378 (2006).
  - [23] G.C. Yong, B.A. Li, L.W. Chen, and W. Zuo, Phys. Rev. C **73**, 034603 (2006).
  - [24] G.C. Yong, B.A. Li, and L.W. Chen, Phys. Rev. C **74**, 064617 (2006) [arXiv:nucl-th/0606003].
  - [25] C. Gale, G. M. Welke, M. Prakash, S. J. Lee, and S. Das Gupta, Phys. Rev. C **41**, 1545 (1990).
  - [26] A.Z. Mekjian, S.J. Lee and L. Zamick, Phys. Rev. C **72**, 044305 (2005); S.J. Lee and A.Z. Mekjian, *ibid.* C **63**, 044605 (2001).
  - [27] M.B. Tsang *et al.*, Phys. Rev. Lett. **86**, 5023 (2001).
  - [28] D. V. Shetty *et al.*, Phys. Rev. C **70**, 011601(R) (2004); D. V. Shetty *et al.*, *ibid.* C **71**, 024602 (2005); D.V. Shetty *et al.*, arXiv:nucl-ex/0603016.
  - [29] G.A. Souliotis *et al.*, Phys. Rev. C **73**, 024606 (2006); J. Igljo *et al.*, *ibid.* C **74**, 024605 (2006); G. A. Souliotis *et al.*, arXiv:nucl-ex/0603006.
  - [30] D.V. Shetty *et al.*, arXiv:nucl-ex/0606032.
  - [31] A. Le Fèvre *et al.* for the ALADIN and INDRA collaborations, Phys. Rev. Lett. **94**, 162701 (2005).
  - [32] W. Trautmann *et al.* for the ALADIN and INDRA collaborations, arXiv:nucl-ex/0603027.
  - [33] S. Kowalski *et al.*, Phys. Rev. C **75**, 014601 (2007).
  - [34] M.B. Tsang *et al.*, Phys. Rev. C **64**, 054615 (2001).



- [35] A.S. Botvina, O.V. Lozhkin and W. Trautmann, Phys. Rev. C **65**, 044610 (2002).
- [36] A. Ono, P. Danielewicz, W.A. Friedman, W.G. Lynch and M.B. Tsang, Phys. Rev. C **68**, 051601(R) (2003); *ibid.* C **70**, 041604 (2004); arXiv:nucl-ex/0507018.
- [37] C.O. Dorso, C.R. Escudero, M. Ison, and J.A. López, Phys. Rev. C **73**, 044601 (2006).
- [38] Y.G. Ma et al., Phys. Rev. C **69**, 064610 (2004); Y.G. Ma et al., *ibid.* C **72**, 064603 (2005); W.D. Tian et al., Chin. Phys. Lett. **22**, 306 (2005).
- [39] C.J. Horowitz and A. Schwenk, Nucl. Phys. **A776**, 55 (2006).